

Theoretical Insights into Heme-Catalyzed Oxidation of Cyclohexane to Adipic Acid

Holger Noack,[†] Valentin Georgiev,[†] Margareta R. A. Blomberg,[†] Per E. M. Siegbahn,[†] and Adam Johannes Johansson^{*‡}

[†]Department of Physics, Albanova, Department of Biochemistry and Biophysics, Arrhenius Laboratories, Stockholm University, S-106 91 Stockholm, Sweden, and [‡]Institut für Organische Chemie, Rheinisch-Westfälische Technische Hochschule (RWTH), Aachen University, Landoltweg 1, D-52056 Aachen, Germany

Received July 14, 2010

Adipic acid is a key compound in the chemical industry, where it is mainly used in the production of polymers. The conventional process of its generation requires vast amounts of energy and, moreover, produces environmentally deleterious substances. Thus, there is interest in alternative ways to gain adequate amounts of adipic acid. Experimental reports on a one-pot iron-catalyzed conversion of cyclohexane to adipic acid motivated a theoretical investigation based on density functional theory calculations. The process investigated is interesting because it requires less energy than contemporary methods and does not produce environmentally harmful side products. The aim of the present contribution is to gain insight into the mechanism of the iron-catalyzed cyclohexane conversion to provide a basis for the further development of this process. The rate-limiting step of the process is discussed, but considering the accuracy of the calculations, it is difficult to ensure whether the rate-limiting step is in the substrate oxidation or in the generation of the catalytically active species. It is shown that the slowest step in the substrate oxidation is the conversion of cyclohexanol to cyclohexane-1,2-diol. Hydrogen-atom transfer from one of the OH groups of cyclohexane-1,2-diol makes the intradiol cleavage occur spontaneously.

1. Introduction

Adipic acid (IUPAC name hexanedioic acid) is the most important dicarboxylic acid for the chemical industry. Its main application is to serve as the starting material for the production of nylon and other polymers (PVC, polyurethane), and in small quantities, it is used as a flavorant or acidulant.¹

Contemporary methods for the production of adipic acid are based on the oxidation of cyclohexane. Initially, cyclohexane is oxidized in air using cobalt or manganese catalysts. The result is a mixture of cyclohexanol and cyclohexanone, referred to as “KA oil” (abbreviation of ketone–alcohol oil). The components of KA oil are further oxidized using nitric acid. Nitric acid is a cheap oxidant, but its use is environmentally disadvantageous because nitrogen oxides (NO_x) are generated in the process. Hence, there is considerable interest in the use of molecular oxygen or hydrogen peroxide,

which would provide a far more environmentally friendly oxidation.^{2–5}

Recently, Zhong and co-workers reported on a homogeneous iron porphyrin catalyzed one-pot conversion of cyclohexane to adipic acid.⁶ The main advantage of this approach is the use of molecular oxygen as the oxidant; furthermore, it requires a lower temperature than contemporary methods and can thus be regarded as a comparatively green process. Unfortunately, the reported yield of adipic acid amounts to 21% only, which is partly due to overoxidation, resulting in the formation of succinic and glutaric acid.⁷ It is thus important to investigate the iron porphyrin catalyzed mechanism of cyclohexane oxidation to gain a better understanding of how adipic acid is formed in the process.

The results reported by Zhong and co-workers are also interesting from bioinorganic and biomimetic perspectives. Iron porphyrin complexes (hemes) are well-known prosthetic groups in a number of metalloproteins—hemoglobin, cytochrome C, P450, peroxidases—whose biological functions range from dioxygen transportation and electron transfer to

*To whom correspondence should be addressed. E-mail: johjo76@gmail.com.

(1) Davis, D. D.; Kemp, D. R. In *Kirk–Othmer Encyclopedia of Chemical Technology*, 4th ed.; Kroschwitz, J. I., Howe-Grant, M., Eds.; Wiley: New York, 1991; Vol. 1, pp 466–493.

(2) Iwahama, T.; Syojo, K.; Sakaguchi, S.; Ishii, Y. *Org. Process Res. Dev.* **1998**, 2, 255–260.

(3) Pigamo, A.; Besson, M.; Blanc, B.; Gallezot, P.; Blackburn, A.; Kozynchenko, O.; Tennison, S.; Crezee, E.; Kapteijn, F. *Carbon* **2002**, 40, 1267–1278.

(4) Raja, R.; Thomas, J. M. *J. Mol. Catal. A: Chem.* **2002**, 181, 3–14.

(5) Saji, P. V.; Ratnasamy, C.; Gopinathan, S. U.S. Patent 6,392,093, 2002.

(6) Yuan, Y.; Ji, H.; Chen, Y.; Han, Y.; Song, X.; She, Y.; Zhong, R. *Org. Process Res. Dev.* **2004**, 8(3), 418–420.

(7) Yuanbin, S. Private communication, Institute of Green Chemistry, Beijing University of Technology, Beijing, China.

redox chemistry. Mononuclear heme and nonheme iron enzymes typically require a cofactor or an external source to provide the electrons necessary to activate the dioxygen molecule for substrate oxidation.^{8,9} Similarly, mononuclear iron(II) porphyrin complexes can activate molecular oxygen via the formation of a diiron peroxide, in which the O–O bond can be cleaved thermally.^{10–15} The O–O bond cleavage results in the formation of a highly reactive ferryl ($\text{Fe}^{\text{IV}}=\text{O}$) species, which is the active oxidant in subsequent substrate oxidation.

The fact that $(\text{Porph})\text{Fe}^{\text{II}}$ complexes can bind and cleave O_2 via the formation of a diiron peroxide was already reported by Balch et al. in the late 1970s.^{10–13} Since then, the reaction has also been studied by Karlin et al.¹⁴ A diiron peroxide, $(\text{Porph})\text{Fe}^{\text{III}}\text{OOFe}^{\text{III}}(\text{Porph})$, that is stable in non-coordinating solvents at -70°C but cleaves the O–O bond upon heating to -30°C is formed. There is therefore no doubt that $(\text{Porph})\text{Fe}^{\text{IV}}=\text{O}$ is formed at the temperature employed in the reaction studied here (140°C).

In the present contribution, the catalytic oxidation of cyclohexane to adipic acid was investigated using hybrid density functional theory (DFT). The suggested mechanism is based on the nowadays well-established reactivity paradigm of the ferryl ($\text{Fe}^{\text{IV}}=\text{O}$) unit.^{16–25} The mechanism consists of three major oxidative steps, each initiated by hydrogen-atom transfer (HAT). First, cyclohexane is oxidized to cyclohexane-1,2-diol via two consecutive hydroxylation steps. Second, cyclohexane-1,2-diol is converted into hexane-1,6-dial (adipaldehyde) by intradiol C–C bond cleavage. Finally, adipaldehyde is oxidized to adipic acid by hydroxylation of the carbonyl groups (Figure 1).

2. Computational Details

All calculations are based on DFT, using the B3LYP hybrid functional.^{26–30} Geometry optimizations, calculations of the final energies, and evaluation of the solvent effects were done

using *Jaguar 5.5/7.0*,³¹ whereas *Gaussian 03*³² was used for optimization of the transition states (TSs) and evaluation of vibrational zero-point effects. All geometry optimizations were done using the double- ζ basis set lacvp, which is composed of the 6-31G description for all light atoms and an effective core potential on iron.³³ Geometries obtained from these calculations are adequate for evaluation of the final energies,^{34,35} which were evaluated using the correlation-consistent polarized triple- ζ basis set cc-pVTZ(-f) (without f functions) on all atoms except iron, for which the triple- ζ lacv3p basis set was used.

Polarization effects of the solvent cyclohexane have been accounted for by employing the self-consistent-reaction-field method at the B3LYP/lacvp level of theory ($\epsilon = 2.0$). The effect of polarization on the reaction energetics is usually small, as long as no substantial charge separation is involved.^{36,37} This is well manifested in the present work, where the computed solvent effects are in all cases smaller than 2 kcal/mol.

Spin populations are used to monitor changes in the spin and oxidation states of the metal ion and were derived from a Mulliken population analysis. Usually, the reported spin density on iron is lower than what would be predicted from formal electron counting and ligand field theory. The reason for this discrepancy is that the unpaired spin density tends to delocalize to the ligand-donor nitrogen atoms.

To reduce the computational cost, the experimentally used ligand *meso*-tetrakis(*o*-chlorophenyl)porphyrin was modeled by an unsubstituted porphyrin ligand. Experimentally, these chlorophenyl substituents are important for solubility of the complex, but it has been shown (for a system with similar ligands on porphyrin) that their effects on the calculated energies of O–O bond cleavage of a diiron peroxide are insignificant.¹⁵ Furthermore, the isomer in which the oxo group is trans with respect to the chlorine atoms is 12.0 kcal/mol more stable than the cis isomer in the preceding peroxo dimer $\text{Fe}^{\text{III}}\text{OOFe}^{\text{III}}$ and 2.1 kcal/mol lower than the cis isomer in the $\text{Fe}^{\text{IV}}=\text{O}$ monomer. Thus, the chlorine substituents are not expected to have any significant influence on the reactions modeled here.

2.1. Reducing the Amount of Hartree–Fock Exchange. It has been shown that reducing the amount of Hartree–Fock exchange

(8) Costas, M.; Mehn, M. P.; Jensen, M. P.; Que, L., Jr. *Chem. Rev.* **2004**, *104*, 939–986.

(9) Sono, M.; Roach, M. P.; Coulter, E. D.; Dawson, J. H. *Chem. Rev.* **1996**, *96*, 2841–2887.

(10) Chin, D.-H.; Del Gaudio, J.; La Mar, G. N.; Balch, A. L. *J. Am. Chem. Soc.* **1977**, *99*, 5486–5488.

(11) Chin, D.-H.; La Mar, G. N.; Balch, A. L. *J. Am. Chem. Soc.* **1980**, *102*, 4344–4350.

(12) Balch, A. L.; Chan, Y. W.; Cheng, R. J.; La Mar, G. N.; Latos-Grazynski, L.; Renner, M. W. *J. Am. Chem. Soc.* **1984**, *106*, 7779–7785.

(13) Balch, A. L. *Inorg. Chim. Acta* **1992**, *198–200*, 297–307.

(14) Ghiladi, R.-A.; Kretzer, R.-M.; Guzei, I.; Rheingold, A.-L.; Neuhold, Y.-M.; Hatwell, K.-R.; Zuberbühler, A.-D.; Karlin, K.-D. *Inorg. Chem.* **2001**, *40*, 5754–5767.

(15) Blomberg, M. R. A.; Johansson, A. J.; Siegbahn, P. E. M. *Inorg. Chem.* **2007**, *46*, 7992–7997.

(16) Shaik, S.; Hirao, H.; Kumar, D. *Acc. Chem. Res.* **2007**, *40*, 532–542.

(17) Hirao, H.; Kumar, D.; Que, L., Jr.; Shaik, S. *J. Am. Chem. Soc.* **2006**, *128*, 8590–8606.

(18) Company, A.; Gomez, L.; Guell, M.; Ribas, X.; Luis, J. M.; Que, L., Jr.; Costas, M. *J. Am. Chem. Soc.* **2007**, *129*, 15766–15767.

(19) Rohde, J. U.; Que, L., Jr. *Angew. Chem., Int. Ed.* **2005**, *44*, 2255–2258.

(20) Klinker, E. J.; Shaik, S.; Hirao, H.; Que, L., Jr. *Angew. Chem., Int. Ed.* **2009**, *48*, 1291–1295.

(21) Altun, A.; Shaik, S.; Thiel, W. *J. Am. Chem. Soc.* **2007**, *129*, 8978–8987.

(22) de Visser, S. P. *Inorg. Chem.* **2006**, *45*, 9551–9557.

(23) Nam, W. *Acc. Chem. Res.* **2007**, *40*, 522–531.

(24) Stone, K. L.; Hoffart, L. M.; Behan, R. K.; Krebs, C.; Green, M. T. *J. Am. Chem. Soc.* **2006**, *128*, 6147–6153.

(25) Derat, E.; Shaik, S. *J. Am. Chem. Soc.* **2006**, *128*, 8185–8198.

(26) Lee, C.; Yang, W.; Parr, R. G. *Phys. Rev. B* **1988**, *37*, 785.

(27) Becke, A. D. *J. Chem. Phys.* **1992**, *96*, 2155.

(28) Becke, A. D. *J. Chem. Phys.* **1992**, *97*, 9173.

(29) Becke, A. D. *J. Chem. Phys.* **1993**, *98*, 5648.

(30) Stephens, P. J.; Devlin, F. J.; Chabalowski, C. F.; Frisch, M. J. *J. Phys. Chem.* **1994**, *98*, 11623.

(31) *Jaguar 5.5/7.0*; Schrödinger, Inc.: Portland, OR, 2007.

(32) Frisch, M. J.; Trucks, G. W.; Schlegel, H. B.; Scuseria, G. E.; Robb, M. A.; Cheeseman, J. R.; Montgomery, J. A., Jr.; Vreven, T.; Kudin, K. N.; Burant, J. C.; Millam, J. M.; Iyengar, S. S.; Tomasi, J.; Barone, V.; Mennucci, B.; Cossi, M.; Scalmani, G.; Rega, N.; Petersson, G. A.; Nakatsuji, H.; Hada, M.; Ehara, M.; Toyota, K.; Fukuda, R.; Hasegawa, J.; Ishida, M.; Nakajima, T.; Honda, Y.; Kitao, O.; Nakai, H.; Klene, M.; Li, X.; Knox, J. E.; Hratchian, H. P.; Cross, J. B.; Bakken, V.; Adamo, C.; Jaramillo, J.; Gomperts, R.; Stratmann, R. E.; Yazyev, O.; Austin, A. J.; Cammi, R.; Pomelli, C.; Ochterski, J. W.; Ayala, P. Y.; Morokuma, K.; Voth, G. A.; Salvador, P.; Dannenberg, J. J.; Zakrzewski, V. G.; Dapprich, S.; Daniels, A. D.; Strain, M. C.; Farkas, O.; Malick, D. K.; Rabuck, A. D.; Raghavachari, K.; Foresman, J. B.; Ortiz, J. V.; Cui, Q.; Baboul, A. G.; Clifford, S.; Cioslowski, J.; Stefanov, B. B.; Liu, G.; Liashenko, A.; Piskorz, P.; Komaromi, I.; Martin, R. L.; Fox, D. J.; Keith, T.; Al-Laham, M. A.; Peng, C. Y.; Nanayakkara, A.; Challacombe, M.; Gill, P. M. W.; Johnson, B.; Chen, W.; Wong, M. W.; Gonzalez, C.; Pople, J. A. *Gaussian 03*, revision D.01; Gaussian, Inc.: Wallingford, CT, 2004.

(33) Hay, P. J.; Wadt, W. R. *J. Chem. Phys.* **1985**, *82*, 299.

(34) Siegbahn, P. E. M. In *Advances in Chemical Physics: New Methods in Computational Quantum Mechanics*; Prigogine, I., Rice, S. A., Eds.; John Wiley & Sons: London, 1996.

(35) Chong, D. P., Ed. *Recent advances in density functional methods*; World Scientific: Singapore, 1997; Part II.

(36) Siegbahn, P. E. M.; Blomberg, M. R. A. *Chem. Rev.* **2000**, *100*, 421.

(37) Siegbahn, P. E. M. *J. Comput. Chem.* **2001**, *22*, 1634.

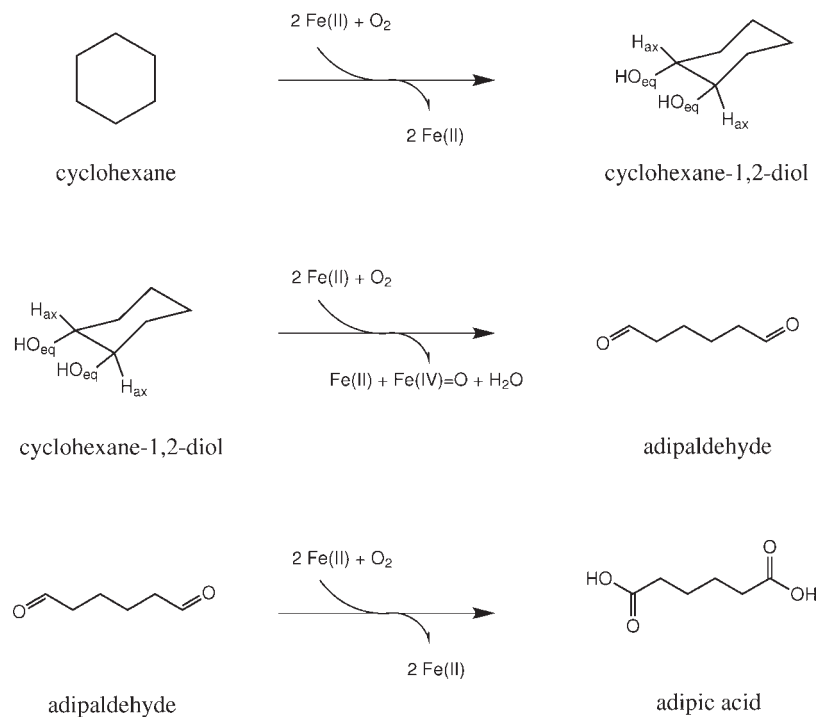


Figure 1. Major oxidative steps in the suggested mechanism for the catalytic conversion of cyclohexane to adipic acid.

from 20% to 15%, as is done in B3LYP*, can give more reliable energies for systems involving transition metals.³⁸ To see the effect of lowering the exchange on the present model system, a few calculations with B3LYP* were done for comparison to B3LYP. In general, high-spin states are destabilized with respect to low-spin states, and this destabilization is proportional to the number of unpaired electrons. During abstraction of a hydrogen atom, the iron atom is reduced from Fe^{IV} to Fe^{III} , and therefore destabilization is larger for the Fe^{III} intermediates than for the reactants. Consequently, destabilization of the TS for HAT is somewhere in between destabilization in the reactant and intermediate. The HAT that initiates the second hydroxylation step is the rate-limiting step involved in the formation of adipic acid from cyclohexanol. The activation energy for this step increases from 17.8 to 22.2 kcal/mol, when the amount of exact exchange is reduced from 20% (B3LYP) to 15% (B3LYP*).

2.2. Effects of Changes in Dispersion and Entropy. A few calculations have been done to test the effect of van der Waals interactions on the reaction energies, using the dispersion-corrected DFT B3LYP-D and the *Orca* package.^{39,40} The effects on the substrate binding/product release were found to be 3–4 kcal/mol, while the effects on the reaction barriers were much smaller (0.5–1.0 kcal/mol).

Entropy effects will also alter the free-energy profile of complex formation and product release, but because the entropy changes associated with solvation are not properly described by the ideal gas partition functions or by the solvation models applied, these values will not be discussed. It should be noted though that, because the effects of dispersion and entropy act in opposite directions on dissociative/associative processes and are of similar size, it is not unreasonable to assume that neglecting both of these effects only gives small errors in the free energy. In other words, for the substrate binding/release, the nondispersion-corrected enthalpy should be rather close to the actual Gibbs free energy. As for the effects of dispersion, entropy effects

Table 1. Calculated Spin Splittings in the Reactant $(\text{Porph})\text{Fe}^{\text{IV}}=\text{O}$ and the Reaction Intermediate Consisting of the $(\text{Porph})\text{Fe}^{\text{III}}\text{OH}$ Complex and the Cyclohexane Radical Resulting from HAT^a

		Mulliken spin				
		M	S_{Fe}	S_{O}	S_{R}	ΔE
$\text{Fe}^{\text{IV}}=\text{O}$						
0 α	1		0.09	-0.10		10.9
2 α	3		1.18	0.85		0.0
4 α	5		3.33	0.49		7.8
$\text{Fe}^{\text{III}}\text{OH/R}^{\bullet}$						
1 α /1 α	3 _{ls}		0.90	0.18	1.02	16.3
1 α /1 β	1 _{ls}		0.97	0.04	-1.02	16.6
3 α /1 α	5 _{is}		2.58	0.43	1.03	11.9
3 α /1 β	3 _{is}		2.56	0.39	-0.99	12.6
5 α /1 α	7 _{hs}		4.00	0.40	-0.96	6.7
5 α /1 β	5 _{hs}		4.00	0.40	-0.96	6.7

^aThe notation 5_{hs} refers to a state of multiplicity 5 (quintet), resulting from antiferromagnetic coupling of the high spin on the iron center and the radical on the substrate. Energies are given in kcal/mol.

on the barrier itself, i.e., with respect to the hydrogen-bonded complex of the catalyst and substrate, should be of minor importance. A similar approach was recently used by Shaik and co-workers.¹⁷

3. Results

The discussion of the suggested mechanism for the oxidation of cyclohexane to adipic acid will be divided into two sections. The first part covers the transformation of cyclohexane to cyclohexane-1,2-diol, and the second part is dedicated to the intradiol C–C bond cleavage in cyclohexane-1,2-diol and the final hydroxylation of hexane-1,6-dial to adipic acid. The catalytically active ferryl species $(\text{Porph})\text{Fe}^{\text{IV}}=\text{O}$ is generated by a reaction between $(\text{Porph})\text{Fe}^{\text{II}}$ and the oxidizing agent O_2 , which was studied earlier.^{10–15} As a

(38) Reiher, M.; Salomon, O.; Hess, B. A. *Theor. Chem. Acc.* **2001**, *107*, 48.

(39) Grimme, S. J. *Comput. Chem.* **2004**, *25*, 1463.

(40) Grimme, S. J. *Comput. Chem.* **2006**, *27*, 1787.

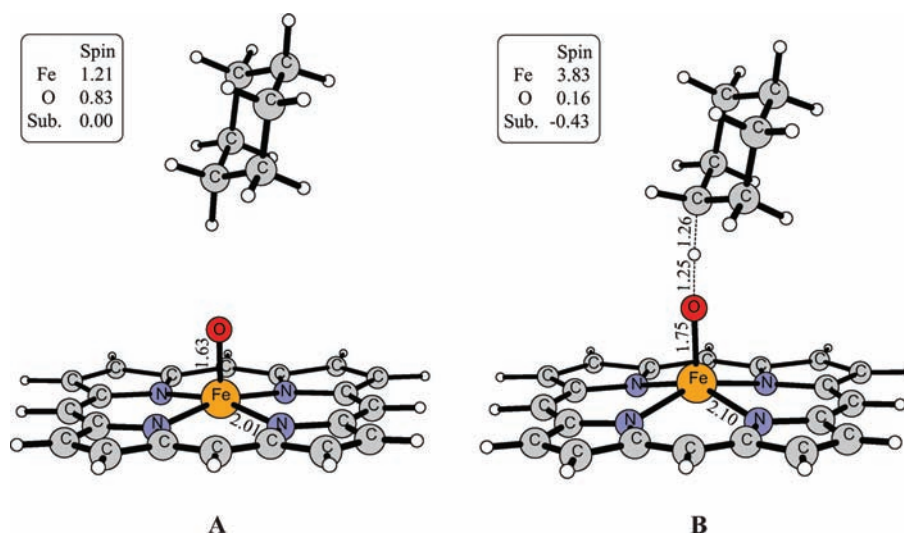


Figure 2. (A) [(Porph)Fe^{IV}(O)/(C₆H₁₂)] reactant complex in its triplet ground state. (B) TS for HAT in the quintet 5_{hs} state. The most important distances and spin populations are given.

consequence of the strong ligand field of the tetradentate porphyrine ligand, the ground state of the (Porph)Fe^{IV}=O reactant complex is a triplet (intermediate-spin configuration on iron; Table 1).

3.1. Conversion of Cyclohexane to Cyclohexane-1,2-diol. **3.1.1. First Hydroxylation Step.** The ground state of the (Porph)Fe^{IV}=O reactant complex remains unaffected by complexation with cyclohexane, i.e., a triplet state in which one of the unpaired electrons is partially delocalized to the oxo group (Figure 2A). The reaction is initiated by HAT from cyclohexane to the FeO group of the reactant complex. During this step, the iron atom is reduced and a radical is created on the cyclohexane molecule, giving an intermediate radical complex [(Porph)Fe^{III}(OH)(C₆H₁₁[•])]. In principle, several different spin states are possible for this intermediate complex, depending on both the spin state of the iron(III) center [high spin (sextet), intermediate spin (quartet), or low spin (doublet)] and the coupling between the unpaired electrons on iron and the substrate radical (antiferromagnetic or ferromagnetic). The energies of the possible states were calculated, and the results are summarized in Table 1. As can be seen in this table, the most important factor determining the energy of this radical intermediate complex is the spin state of iron, with the high-spin state lowest in energy and the low-spin state highest. The coupling between the iron spin and the substrate spin is very weak, yielding essentially the same energy for ferro- and antiferromagnetic coupling. Exploratory calculations showed that only the lowest triplet (3_{is}) and quintet (5_{hs}) states can play any role in the present reactions, and these states are therefore the only ones discussed in the following.

The HAT leading from the triplet ground state to the triplet radical intermediate, 3_{is} , has a barrier of 17.2 kcal/mol. However, the lowest barrier of 13.6 kcal/mol is found for high-spin iron on the quintet, 5_{hs} , surface (Figure 2B).

Because the quintet state is 7.8 kcal/mol higher than the triplet ground state in the reactant, the system has to

undergo a spin crossing before reaching the TS (Figure 3). This behavior is typical for reduction of the Fe^{IV}=O group in strong ligand fields.^{17,41}

The formation of the intermediate radical complex (Porph)Fe^{III}(OH)/(C₆H₁₁[•]) in the reactive quintet state, 5_{hs} , is endothermic with 6.7 kcal/mol with respect to the reactant ground state. The corresponding ferromagnetically coupled quintet state involving intermediate spin on iron, 5_{is} , lies 5.2 kcal/mol higher (Table 1). The reaction proceeds via radical recombination between the radical substrate and the OH group on iron, and as a consequence of the exothermicity for this reaction ($\Delta H = -37.0$ kcal/mol), the barrier for this step is very low (0.7 kcal/mol). A second spin crossing from the reactive quintet state to the triplet ground state of the iron(II) product occurs that increases the exothermicity by another 5 kcal/mol. The final dissociation of cyclohexanol is easily feasible because it is only weakly coordinated to the (Porph)Fe^{II} complex ($\Delta H = 1.3$ kcal/mol).

3.1.1. Second Hydroxylation Step. Further hydroxylation of cyclohexanol requires a new reactive (Porph)Fe^{IV}=O complex. The spin splitting between the triplet ground state and the quintet (7.7 kcal/mol) and singlet (9.5 kcal/mol) excited states remains almost unaffected by the hydrogen bond between cyclohexanol and the FeO group (Table 2).

As for hydroxylation of cyclohexane to cyclohexanol, the system undergoes a spin crossing to the quintet state before reaching the TS for HAT. Starting from the hydrogen-bonded ground-state complex (Figure 4A), the HAT in the ortho-equatorial position has a barrier of 17.8 kcal/mol in the reactive quintet state (Figure 5). This barrier is thus 4.2 kcal/mol higher than that of the HAT in hydroxylation of cyclohexane to cyclohexanol. However, if compared to the separated reactants, the HAT initiating the hydroxylation of cyclohexanol would have a barrier of only 9.5 kcal/mol, which is 4.1 kcal/mol lower than the HAT in the hydroxylation of cyclohexane. The reason for the higher HAT barrier in the hydroxylation of cyclohexanol is due to the hydrogen bond that has a larger stabilizing effect on the reactant complex than on the TS.

(41) Schröder, D.; Shaik, S.; Schwarz, H. *Acc. Chem. Res.* **2000**, *33*, 139–145.

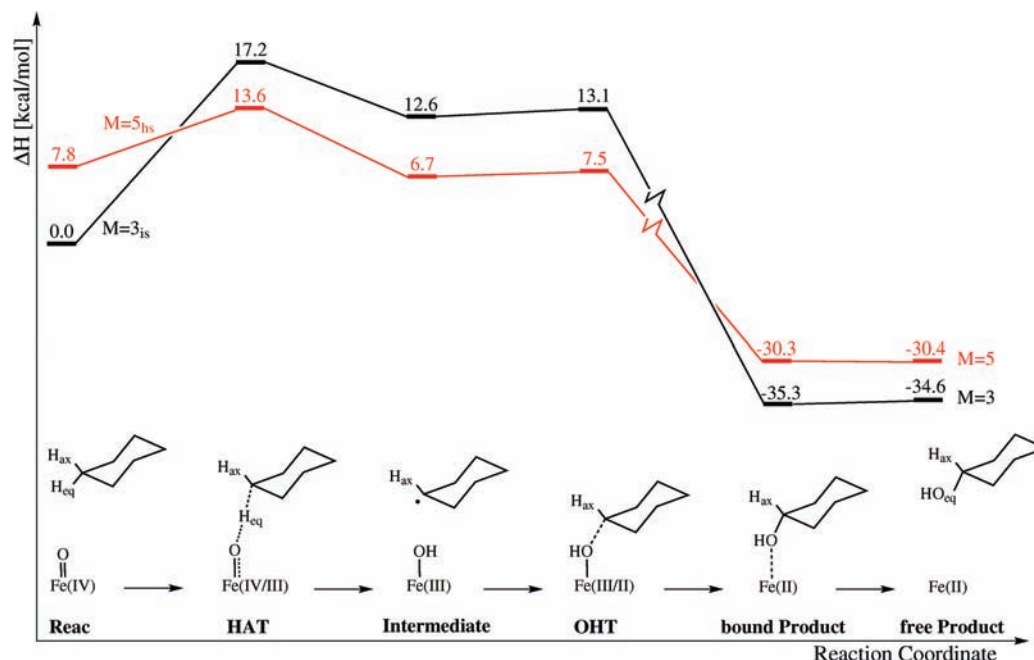


Figure 3. Energy profile for the iron-catalyzed oxidation of cyclohexane to cyclohexanol.

Table 2. Summary of the Energetic Spin Splittings for Reactants (Reac), Reactant–Substrate (RS) Complex, HAT Barriers, Radical Intermediates (Int), and Hydroxylation (OHT) Barriers of the First Two Hydroxylation Steps in the Oxidation of Cyclohexane to Cyclohexane-1,2-diol^a

	energetic spin splittings					
	<i>M</i>	Reac	RS	HAT	Int	OHT
first hydroxylation step	1	10.9 (10.7)				
	3 _{is}	0.0 (0.0)		17.2 (19.0)	12.6 (16.8)	13.1 (16.7)
	5 _{hs}	7.8 (10.6)		13.6 (17.6)	6.7 (13.5)	7.5 (13.8)
second hydroxylation step	1	9.5 (9.2)				
	3 _{is}	0.0 (0.0)	−8.3 (−8.6)	12.5 (14.0)	3.5 (7.7)	8.3 (11.3)
	5 _{hs}	7.7 (10.6)	−0.6 (3.0)	9.5 (13.6)	0.3 (7.2)	3.4 (8.6)

^a The notation 5_{hs} refers to a state of multiplicity 5 (quintet), resulting from antiferromagnetic coupling of the high spin on the iron center and the radical on the substrate. Energies are given in kcal/mol. B3LYP* energies are given in parentheses.

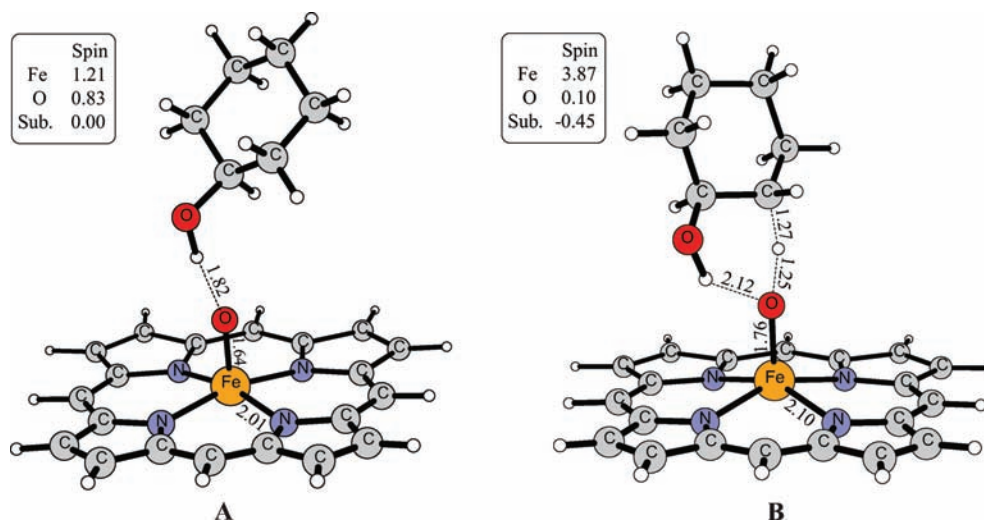


Figure 4. (A) [(Porph)Fe^{IV}(O)/(C₆H₁₁OH)] reactant complex in its triplet ground state. (B) TS for HAT in the reactive quintet state. The most important distances and spin populations are given.

A radical intermediate is formed with an endergonicity of 8.6 kcal/mol with respect to the hydrogen-bonded triplet ground state of the reactant complex (Figure 5). The barrier for the subsequent radical recombination is

only 3.1 kcal/mol and leads to the formation of cyclohexane-1,2-diol with an exothermicity of −35.1 kcal/mol. As before, the system crosses back to the triplet state during the hydroxylation step. Cyclohexane-1,2-diol is

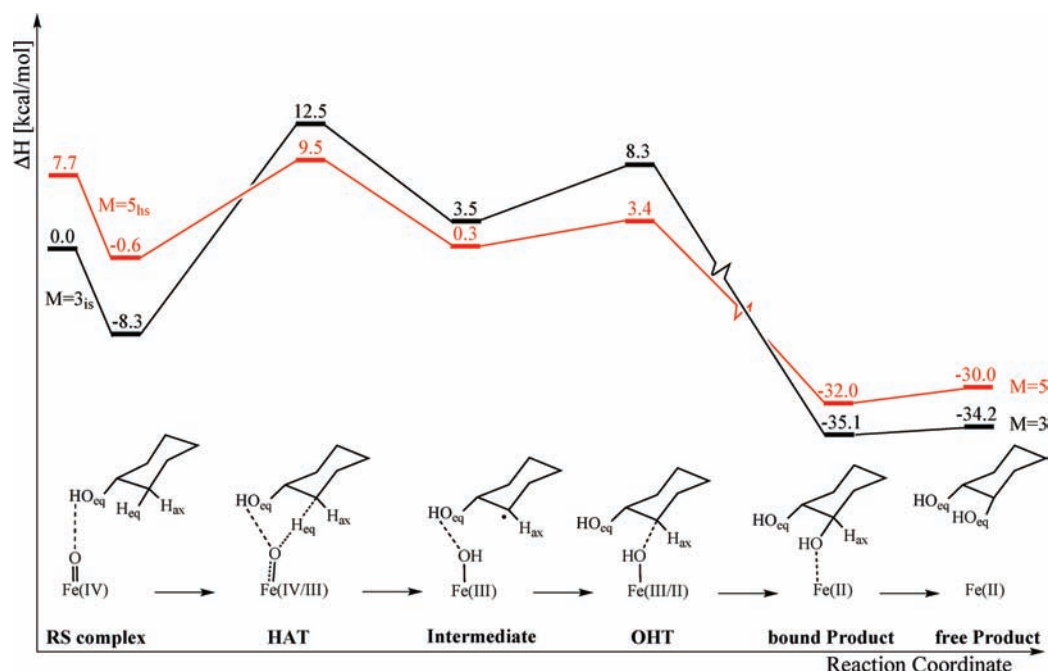


Figure 5. Energy profile for hydroxylation of cyclohexanol to cyclohexane-1,2-diol.

only weakly coordinated to the (Porph)Fe^{II} complex (0.9 kcal/mol).

The resulting cyclohexane-1,2-diol has both neighboring OH groups in equatorial positions. Two other conformations are possible for ortho substitution: one of the OH groups in an equatorial position and the other one in an axial position or both OH groups in axial positions. It was found that the barrier for HAT is lowest for generation of the diequatorial conformation. Furthermore, the diequatorial conformation was 1.2 kcal/mol more stable than the equatorial–axial conformation and 3.5 kcal/mol more stable than the diaxial conformation.

A final note can be made on the effects of reducing the amount of Hartree–Fock exchange, from 20% used in B3LYP to 15% used in B3LYP* (Table 2). As explained in the Computational Details section, there are two distinct effects. One effect is destabilization of high-spin states with respect to low-spin states. In Table 2, this can be seen, for example, in the reactant of the first hydroxylation, for which the triplet is the ground state and the triplet–quintet splitting increases from 7.8 to 10.6 kcal/mol. In the reaction intermediate, the quintet is the ground state and the quintet–triplet splitting instead decreases from 5.9 to 3.3 kcal/mol when the amount of Hartree–Fock exchange is reduced (Table 2). The second effect of reducing the amount of Hartree–Fock exchange is associated with the reduction/oxidation of the metal center. For the first hydroxylation step, B3LYP predicts the HAT to be endothermic with 12.6 kcal/mol in the triplet state (Table 2). The endothermicity in the triplet state increases to 16.8 kcal/mol when B3LYP* is used; i.e., the HAT in the triplet state becomes 4.2 kcal/mol more endothermic when the amount of Hartree–Fock exchange is reduced. The corresponding effect in the quintet state is slightly smaller, 4.0 kcal/mol. Interestingly, these effects are identical for the HAT of the second hydroxylation step (Table 2). In the TS of HAT, both effects discussed above come into play because (1) a spin crossing occurs before the HAT TS

and (2) iron is being reduced. When the amount of Hartree–Fock exchange is reduced, the barrier for the first HAT increases by 4.0 kcal/mol (with respect to the separated species). The corresponding effect on the HAT of the second hydroxylation step is 4.4 kcal/mol, with respect to the hydrogen-bonded complex (Table 2). In summary, reducing the amount of Hartree–Fock exchange has effects on the calculated reaction energies and barriers, but it does not change the general picture.

3.2. C–C Bond Cleavage and Adipic Acid Formation.

Both the equatorial OH groups of cyclohexane-1,2-diol can form hydrogen bonds with the oxo group of the (Porph)Fe^{IV}=O complex (Figure 6A). Such a hydrogen-bonded complex is only –4.0 kcal/mol more stable than the separated reactants and is thus only half as stable as the corresponding hydrogen-bonded reactant complex with cyclohexanol (Figure 4A). This is explained by the fact that free cyclohexane-1,2-diol has an internal hydrogen bond that is broken upon hydrogen bonding to (Porph)Fe^{IV}=O, which partly cancels the energy gain of complexation.

The intradiol C–C bond cleavage is initiated by HAT from one of the substrate OH groups to the ferryl group (Figure 6B). The barrier for this OH HAT is 10.2 kcal/mol in the reactive quintet state; it is thus significantly lower than the barrier for the above-described CH HAT. The radical intermediate formed after this initial HAT (Figure 6C) is very unstable with respect to C–C bond dissociation, which is concerted with a second HAT from the remaining hydroxide of the radical substrate to the (Porph)Fe^{III}OH complex (Figure 6D). In the gas phase, the calculated barrier for this step is only 1.8 kcal/mol. However, when dielectric solvent effects and vibrational zero-point corrections are added, the energy of the optimized TS is lowered to 5.4 kcal/mol below the radical intermediate. Therefore, it can be concluded that after the initial OH HAT the system proceeds toward the formation of hexane-1,6-dial without further barriers

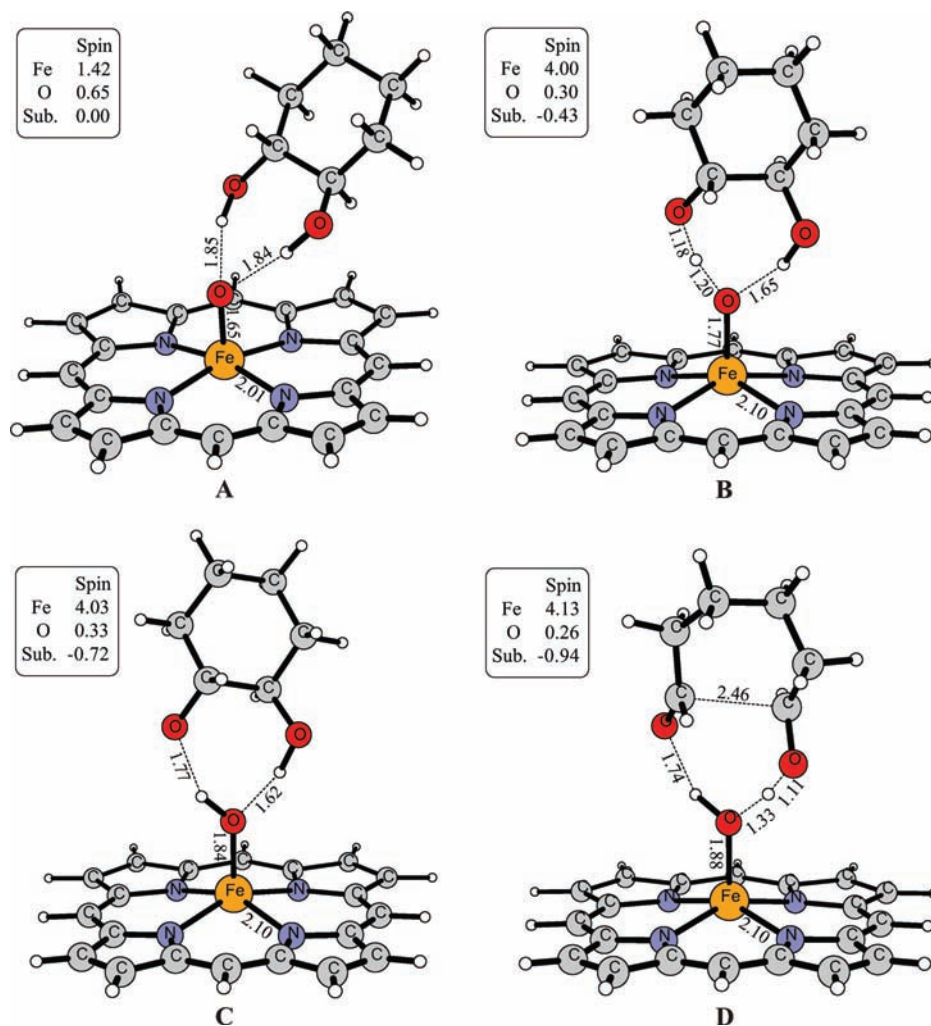


Figure 6. (A) Reactant complex $(\text{Porph})\text{Fe}^{\text{IV}}=\text{O}/\text{C}_6\text{H}_{10}(\text{OH})_2$ in its triplet ground state. (B) TS for HAT in the quintet state. (C) Reaction intermediate complex $(\text{Porph})\text{Fe}^{\text{III}}(\text{OH})/\text{C}_6\text{H}_{10}(\text{OH})\text{O}^*$ in the quintet state. (D) Concerted TS for C–C bond cleavage and the second HAT in the quintet state.

(Figure 7). A hypothetical, more symmetric, and concerted TS, in which both of the hydrogen atoms are transferred simultaneously to the FeO group along with intradiol C–C bond cleavage, was carefully searched for but could not be located.

The conversion of cyclohexane-1,2-diol to adipaldehyde is very exothermic ($\Delta H = -36.1$ kcal/mol) and the product is only weakly hydrogen-bonded ($\Delta H = 3.5$ kcal/mol) to the resulting $(\text{Porph})\text{Fe}^{\text{II}}(\text{H}_2\text{O})$ complex. The water molecule of the product complex has a binding enthalpy of 9 kcal/mol and could thus be a potential inhibitor on the catalytic activity of $(\text{Porph})\text{Fe}^{\text{II}}$. However, it is likely that the equilibrium of water dissociation is shifted toward the free species when entropy effects are considered.

The final steps toward the formation of adipic acid consist of two similar, consecutive hydroxylations of the adipaldehyde carbonyl groups. The chemistry involved follows the $\text{Fe}^{\text{IV}}=\text{O}$ reactivity pattern described for the preceding hydroxylation steps, i.e., C–H hydrogen abstraction and subsequent hydroxylation via radical recombination. However, in this case the hydrogen atom comes from a carbonyl group, for which the radical state is more stable than an aliphatic carbon radical. For this reason, the HAT barriers are much lower than the barriers for aliphatic C–H abstraction.

The first HAT from adipaldehyde has a barrier of only 7.7 kcal/mol in the reactive quintet state. Similarly, the HAT from 6-oxohexanoic acid has a barrier of 8.2 kcal/mol. In both cases, the subsequent hydroxylation has a much lower barrier with 3.2 and 1.8 kcal/mol, respectively. These two final oxidations are the most exothermic of all of the steps discussed so far: -58.8 kcal/mol for the formation of 6-oxohexanoic acid and -57.4 kcal/mol for adipic acid. An overview of the investigated pathway is presented in Figure 8.

3.3. Comparison with Experiment. At the present state, the iron-catalyzed oxidation of cyclohexane to adipic acid is not very selective (21%). The main byproducts formed during the reaction are cyclohexanol, cyclohexanone, succinic acid, glutaric acid, cyclohexylhydroperoxide, and cyclohexyl adipate.⁷ Cyclohexanol is formed in the pathway explored here, while cyclohexanone is likely to form by transfer dehydrogenation from cyclohexanol to the ferryl group. The shorter dicarboxylic acids (succinic and glutaric acid) are formed by overoxidation of adipic acid, which is difficult to avoid because of the strong thermodynamic driving force for aliphatic oxidation by the $(\text{Porph})\text{Fe}^{\text{IV}}=\text{O}$ group.

The slowest step along the reaction pathway explored here is the HAT initiating the hydroxylation of

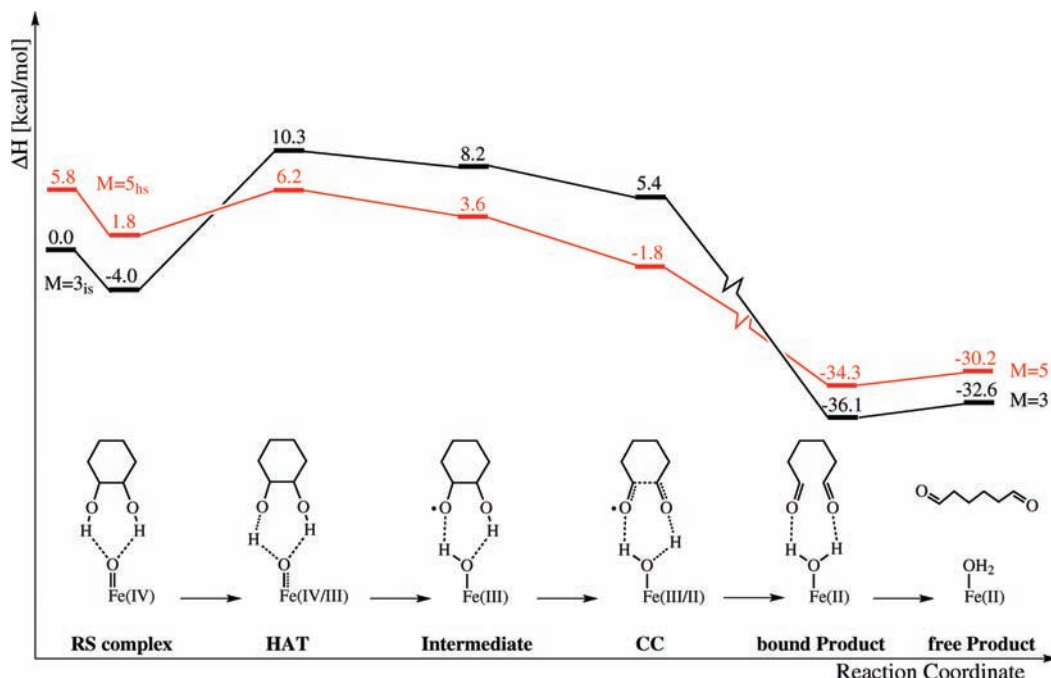


Figure 7. Energy profile for the oxidation of cyclohexane-1,2-diol to 1,6-hexanedial via intradiol C–C cleavage.

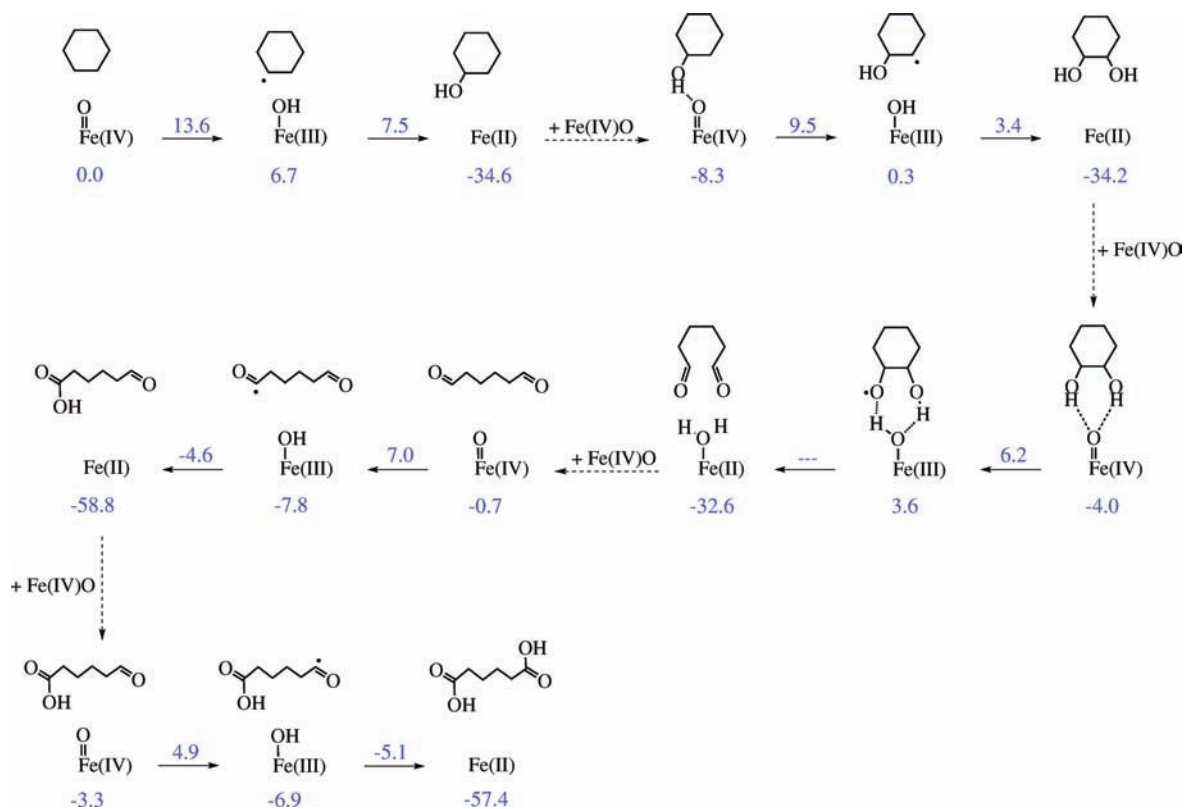


Figure 8. Complete mechanism for the conversion of cyclohexane to adipic acid. Because the thermodynamics for the $\text{Fe}^{\text{IV}}=\text{O}$ formation are unknown, each of these consecutive series has the separated reactant/substrate species as a reference point.

cyclohexanol to cyclohexane-1,2-diol. The calculated energy barrier for this step is predicted to be between 17.8 (B3LYP) and 22.2 (B3LYP*) kcal/mol, depending on the amount of exact exchange used in the hybrid density functional. This barrier can be compared to the kinetics of $(\text{Porph})\text{Fe}^{\text{IV}}=\text{O}$ generation from $(\text{Porph})\text{Fe}^{\text{II}}$ and

O_2 , which has been determined experimentally. The measured activation parameters ($\Delta H^\ddagger = 14.5$ kcal/mol; $\Delta S^\ddagger = -15$ cal/mol) give a free energy barrier of 17.4 kcal/mol at -80 °C,¹¹ which, in turn, corresponds to a barrier of 20.7 kcal/mol at 140 °C. These results indicate that the rate-limiting step in the oxidation of cyclohexane

to adipic acid might not be the substrate oxidation itself but possibly generation of the (Porph)Fe^{IV}=O oxidant. This aspect is interesting because it is known that generation of the (Porph)Fe^{IV}=O from (Porph)Fe^{II} and O₂ is significantly faster when an iron-coordinating Lewis base is added to the reaction solution.¹⁴ Thus, if generation of the ferryl oxidant is the rate-limiting step, it could be possible to run the reaction at a lower temperature in the presence of a Lewis base, which could have positive effects on the selectivity. However, regarding the uncertainties in the computed activation energy for the substrate oxidation, the question of the rate-determining step must be left as an open question for further experimental and computational studies to answer.

4. Conclusions

As reported by Zhong and co-workers, adipic acid is formed in a solution of (Porph)Fe^{II} in cyclohexane, under oxygen pressure and rather mild conditions. Although the yield of adipic acid is low (21%), the process is interesting because it is comparatively environmentally friendly.

On the basis of the reactivity paradigm of the ferryl group (Fe^{IV}=O), a mechanism is proposed and investigated using DFT calculations. The first transformation in this mechanism is the conversion of cyclohexane to cyclohexane-1,2-diol, which occurs via two consecutive hydroxylation steps. These hydroxylations are initiated by HAT from the substrate to the (Porph)Fe^{IV}=O oxidant, followed by rebinding of the iron OH group and the carbon radical. The slowest step

along this path is found to be the C–H hydrogen abstraction that initiates the hydroxylation of cyclohexanol to cyclohexane-1,2-diol. The reason that this particular HAT has a higher barrier than the other HAT steps can be found in the formation of a rather stable hydrogen-bonded complex. The absolute value of the activation energy is somewhat uncertain from the calculations because it increases from 17.8 to 22.2 kcal/mol when the amount of exact exchange is reduced from 20% (B3LYP) to 15% (B3LYP*).

In the following part of the mechanism, cyclohexane-1,2-diol is converted to adipaldehyde. This is initiated by a hydrogen-atom abstraction from one of the substrate OH groups, after which intradiol C–C bond cleavage occurs spontaneously along with transfer of a second hydrogen atom from the remaining OH group of the substrate. The reaction is completed by oxidation of adipaldehyde to adipic acid via two consecutive hydroxylations with low energy barriers.

Finally, it is interesting to note that earlier experimental and computational studies^{11,15} have indicated that the barrier for O–O cleavage in a diiron peroxide is higher than 20 kcal/mol. It is thus possible that the rate-limiting step in the oxidation of cyclohexane to adipic acid is not the substrate oxidation itself but generation of the active oxidant (Porph)Fe^{IV}=O.

Supporting Information Available: Optimized structures for reactants, TSs, and intermediates. This material is available free of charge via the Internet at <http://pubs.acs.org>.